

Effect of Pulsed Electromagnetic Field (PEMF) on Infarct Size and Inflammation After Cerebral Ischemia in Mice

Juan Carlos Pena-Philippides · Yirong Yang ·
Olga Bragina · Sean Hagberg · Edwin Nemoto ·
Tamara Roitbak

Received: 18 November 2013 / Revised: 9 January 2014 / Accepted: 3 February 2014
© Springer Science+Business Media New York 2014

Abstract Pulsed electromagnetic fields (PEMF) have been demonstrated to have anti-inflammatory and pro-regenerative effects in animals and humans. We used the FDA-approved Sofpulse™ (Ivivi Health Sciences, LLC) to study effect of PEMF on infarct size and poststroke inflammation following distal middle cerebral artery occlusion (dMCAO) in mice. Electromagnetic field was applied within 30–45 min after ischemic brain damage and utilized twice a day for 21 consecutive days. Ischemic infarct size was assessed using MRI and histological analysis. At 21 days after dMCAO, the infarct size was significantly (by 26 %) smaller in PEMF-treated animals as compared to controls. Neuroinflammation in these animals was evaluated using specialized cytokine/chemokine PCR array. We demonstrate that PEMF significantly influenced expression profile of pro- and anti-inflammatory factors in the hemisphere ipsilateral to ischemic damage. Importantly, expression of gene encoding major pro-inflammatory cytokine IL-1 α was significantly reduced, while expression of major anti-inflammatory IL-10 was significantly increased. PEMF application significantly downregulated genes encoding members of the major pro-apoptotic tumor necrosis factor (TNF) superfamily indicating that the treatment could have both anti-inflammatory and anti-apoptotic effects. Both reduction of infarct size and influence on neuroinflammation could have a potentially important positive impact on the

poststroke recovery process, implicating PEMF as a possible adjunctive therapy for stroke patients.

Keywords Pulsed electromagnetic field · dMCAO · Ischemic infarct · Neuroinflammation

Introduction

Stroke is a major public health problem with 750,000 cases in the USA and 15 million worldwide each year [1], as well as a leading cause of serious, long-term disability in the USA with about 6.5 million survivors [2]. The associated ischemic damage involves cellular bioenergetic failure, excitotoxicity, oxidative stress, blood–brain barrier dysfunction, microvascular injury, postischemic inflammation, and ultimately, the death of the endothelial cells, neurons, and glia [3]. All these events lead to permanent cerebral injury in the center (core) of the ischemic region.

Stroke is followed by acute and prolonged inflammatory response including the activation of glial cells, production of inflammatory cytokines, and infiltration of monocytes into the brain [4]. Initial stage of poststroke inflammatory process is triggered and regulated by various cytokines, such as interleukins-1 alpha and beta (IL-1 α and IL-1 β), interleukin-6 (IL-6), interleukin-10 (IL-10), and tumor necrosis factor alpha (TNF- α). Original elevation of cytokine expression starts as early as several hours and peaks at 3–4 days after stroke. This molecular inflammation is followed by cellular inflammatory response, resulting in activation and recruitment of different types of cells into the ischemic area, including neutrophils, lymphocytes, monocytes, microglia, and astrocytes [5]. Cellular inflammation, associated with additional release of pro-inflammatory factors by the activated microglia and astrocytes, can last for up to several weeks after stroke [6]. It is widely accepted that these events contribute to brain

J. C. Pena-Philippides · O. Bragina · E. Nemoto · T. Roitbak (✉)
Department of Neurosurgery, University of New Mexico Health
Sciences Center, 1101 Yale Blvd, Albuquerque
NM 87106-3834, USA
e-mail: troitbak@salud.unm.edu

Y. Yang
Brain Imaging Center and College of Pharmacy, University of New
Mexico, Albuquerque, NM, USA

S. Hagberg
Rio Grande Neurosciences, LLC, San Francisco, CA, USA

injury: lower levels of pro-inflammatory cytokines and higher expression of anti-inflammatory cytokines are related to lower infarct size and a better clinical outcome [5, 7]. On the other hand, however, inflammatory cytokines can participate in the initiation of the restorative processes and tissue remodeling following brain damage. Pro-inflammatory cytokines and chemokines can activate neuroprotective pathways as well as initiate neural stem cell migration and activation/differentiation [6, 8].

Poststroke survival has significantly improved over the years and yet treatment directed toward recovery remains limited. Traditional approach utilizing treatment with tissue-plasminogen activator (rt-PA) for thrombolysis is associated with time limitations (3-h therapeutic window) and complications, including a risk of hemorrhage, and the potential damage from reperfusion/ischemic injury [7]. Neurorestorative processes may be enhanced by the improvement of ischemia-induced cerebral angiogenesis using pro-angiogenic factors or enhancement of neurogenesis using stem cell therapy. However, utilization of pro-angiogenic molecules may also be accompanied by an increase in vascular permeability and edema, and cell-based approaches can be accompanied by a number of other complications, such as transplant rejection or tumor formation. The present study focuses on entirely different approach to poststroke regeneration: a noninvasive treatment with pulsed electromagnetic field.

Pulsed electromagnetic fields (PEMF) from low- to pulse-modulated radio frequencies have been successfully employed as adjunctive therapy for wide range of clinical conditions. PEMF signals represent short bursts of electrical current, generated by relatively simple devices, allowing an external, non-invasive application to injured tissue, without producing heat or interfering with nerve or muscle function [9]. Exposure to pulsed electromagnetic field has been shown to attenuate tissue damage following stroke: PEMF stimulation decreased infarct size after transient focal ischemia in rabbits [10]. Certain beneficial effect of PEMF application on visual memory was reported in Alzheimer patients [11]. Significant improvements in Parkinsonian motor symptoms were also seen following repetitive treatments with AC pulsed electromagnetic fields [12]. An accumulated scientific data support an idea of therapeutic effect of electromagnetic fields in inflammatory diseases and conditions [13]. The anti-inflammatory effects of the FDA-approved PEMF treatment parameters have been demonstrated by a decrease in inflammatory IL-1 β cytokine after traumatic brain injury in rats [14], decrease in pain and IL-1 β after breast reduction [15], and pain reduction after breast augmentation [16] and osteoarthritis [17].

In the present study, we investigated possible beneficial influence of PEMF treatment on infarct size and post-injury inflammation at different time points following experimental cerebral ischemia in mice.

Materials and Methods

Distal Middle Cerebral Artery Procedure The experimental procedures were approved by the University of New Mexico Office of Animal Care Compliance. All institutional and national guidelines for the care and use of laboratory animals were followed. Distal middle cerebral artery occlusion (dMCAO) was performed on 2-month-old C57BL/6 mice. The MCA was exposed via transtemporal approach [18]. The mice were anesthetized using isoflurane gas (induction dosage 2–3 %; maintenance dosage 1.5–2 %) and a mixture of O₂:N₂O gases in the ratio 2:1, delivered during the surgery. A small burr hole (located 1 mm rostral to the fusion of zygoma and squamosal bone, and 3 mm ventral to the parietal bone) was made, and the MCA was coagulated with low-heat electrocautery (Bovie Medical, FL). After that, animals were allowed to undergo recovery.

Treatment (PEMF Administration) PEMF signal was a 27.12-MHz carrier modulated by a 2-ms burst repeating at 2 bursts/s (2 Hz). The signal amplitude was adjusted to provide 3 \pm 0.6 V/m within the mouse brain. The PEMF exposure chamber was constructed such that free roaming mice were restricted to this field amplitude. PEMF field characteristics were verified with a calibrated shielded loop probe 1 cm in diameter (model 100A, Beehive Electronics, Sebastopol, CA) connected to a calibrated 100-MHz oscilloscope (model 2012B, Tektronix, Beaverton, OR). In the previous studies, measurement of the PEMF signal distribution in a tissue phantom and in air showed that PEMF amplitude dose was uniform to within \pm 20 %. An additional measure in the tissue phantom showed that the Specific Absorption Rate (SAR), a measure of peak RF power in tissue, was 40 mW/kg, which is well below the level at which detectable temperature rise could occur in the tissue target [9]. PEMF and control treatments started within 30–45 min after dMCAO surgery (as the animals recovered from anesthesia). Animals from the treatment (PEMF-treated) group were subjected to 15-min PEMF administration, two times daily, with 4-h interval between the treatment sessions. Control group was subjected to 15 min of control treatment (“null” signal) by switching to “sham” mode of the applicator. The groups were treated for 21 consecutive days. After completion of 21 full days of treatment, the animals were sacrificed and the brains were prepared for histological evaluation. For the assessment of neuroinflammation, PEMF treatment (with described above regiment) was initiated either immediately or at 3 days after dMCAO, and samples were collected either at 4 or 7 days after dMCAO (4 days of PEMF treatment was applied in both cases).

Animal Groups 24 C57BL/6 male mice (2 months old, Jackson Laboratories) were subjected to dMCAO. Two experimental groups—PEMF-treated and control groups were generated (12 mice/group). It is important to note that PEMF treatment parameters used for this study are similar to PEMF

devices currently in clinical use for their FDA-cleared use, treatment of postoperative pain and edema and for treating chronic wounds (a Medicare approved use). There are no known side or adverse effects of PEMF in human or rodent populations.

MRI Infarct size was evaluated using MRI at 24 h, 7 days, 14 days, and 21 days after dMCAO, in order to detect the extent of the brain damage within control and PEMF-treated animals. The MRI examinations were performed on 4.7T Biospec® dedicated research MR scanner (Bruker Biospin; Billerica) equipped with a single tuned surface coil for mouse brain (RAPID Biomedical, Rimpur). The mice were anesthetized using isoflurane gas (induction dosage 2–3 %; maintenance dosage 1.5–2 %) and a mixture of O₂:N₂O gases in the ratio 2:1, delivered during the measurements. Real-time monitoring of physiological parameters (heart rate and respiratory rate) was performed during the entire duration of the study. A tri-pilot scan using gradient echo sequence was used to acquire initial localizer images. T2-weighted MRI was performed with a fast spin-echo sequence (RARE), TR/TE=5,000/56 ms, FOV=4 cm×4 cm, slice thickness=1 mm, interslice distance=1 mm, number of slices=12, matrix=256×256, number of average=3.

Infarct Volume Infarct volume was calculated based on the widely used method proposed in [19], using Image J analysis software. The optical density threshold was determined for the gray matter in the unlesioned control hemisphere in each slice, and used for the recognition of normal gray matter in the lesioned hemisphere. The areas of noninfarcted (normal) brain tissue were measured in control (C) and lesioned (L) hemispheres, in each T2-weighted MRI slice. The measured areas were summarized, and the respective V_C and V_L volumes were calculated by multiplying each sum by the distance between slices (1 mm). The infarction volume was expressed as a percentage of the volume of the control hemisphere, using the following formula: $\%I=100 \times (V_C - V_L) / V_C$.

Histochemical Evaluation of the Infarct Size At 21 days after dMCAO, PEMF-treated and control animals were subjected to heart perfusion, and the brains were processed for tissue cryosectioning. 8 serial (35 mm thick) coronal sections/mouse ($N=6$ mice per group) were used to assess the brain damage. Brain sections were stained with thionine and imaged using Zeiss stereomicroscope and AxioVision software. Since the necrotic tissue disappears at the later stages after dMCAO (due to development of cystic zone), the whole brain lesion volume was measured according to the indirect method by assessing the size differences between the remaining ipsilateral and unlesioned contralateral hemispheres. On each section, the areas of both hemispheres were measured using Image J software. The infarction of the remaining tissue in the lesioned hemisphere was detected by the lightly (or unstained) regions of the thionine-

stained section. The infarct area and volume were calculated as described for the MRI-based measurements.

Assessment of Cytokine/Chemokine Expression Profiles Two to three brains per each group were used to generate separate sample duplicates or triplicates for this analysis. For these experiments, brain cortices were dissected and stored in RNAlater solution (Ambion). Total RNA was isolated using RNeasy kit (Qiagen), from the hemispheres ipsilateral to dMCAO injury. PCR Array experiments were performed in collaboration with the UNM CUGR UNM Affymetrix facility and Qiagen Company, according to the manufacturer's recommendations. The obtained raw data were analyzed using RT² Profiler software (Qiagen). Only the genes with consistent expression levels (within the duplicate or triplicate samples) were picked up for statistical analysis. The fold changes of gene expressions (treatment vs control) were calculated and the transcripts that showed greater than a 1.5-fold change in expression (either up- or downregulated) were retained.

At the final step, statistical significance (P value<0.05) and reliability of the results was automatically evaluated.

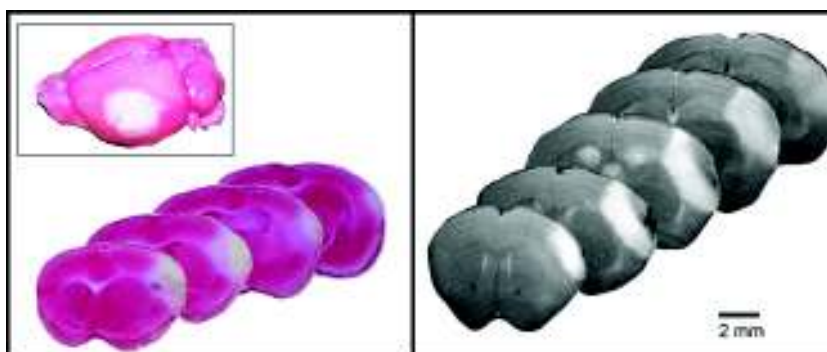
Results

PEMF Treatment Reduces the Infarct Size at 21 Days Following dMCAO

The effect of PEMF treatment on ischemia-induced infarct size was studied using (direct) dMCAO as an experimental model of cortical ischemia (Fig. 1). This model produces an infarct in the frontal and parietal cortex, which over time progresses into adjacent temporal, frontal, and cingulate cortex and dorsolateral striatum [18, 20, 21]. The brain damage progresses from vasogenic edema at 24 h to tissue infarction at 7 and 14 days and significant brain tissue resorption at 21 days. Besides its high reproducibility and survival rate, the advantage of this model is that it produces smaller infarct comparable to human stroke [21]. PEMF and control treatments were initiated at 3–45 min after dMCAO (right after the animals recovered from surgery) and lasted for 21 days (15 min, 2× per day, with 4 h interval).

MRI-Based Measurements of Infarct Size After dMCAO Brain tissue damage after dMCAO was evaluated using MRI as described in “Materials and Methods.” T2-weighted MRI-based measurements of the infarct volume were done at 24 h, 7 days, 14 days, and 21 days post-dMCAO. Infarct volume was measured and calculated according the methods described in [19, 22]. The calculations were performed based on the damaged area in each slice and the distance between slices. These volumes were corrected for brain swelling/shrinkage as described by Swanson et al. (1990) and were

Fig. 1 Description of dMCAO model in mice: TTC staining (*left panel*) and MRI images were performed at 24 h after dMCAO. These representative images demonstrate dMCAO-associated lesions characteristic for this post-injury time period, involving mostly somatosensory cortex and part of the white matter. *Bar*, 2 mm



expressed in percent of the intact (contralateral to dMCAO-induced damage) hemisphere.

dMCAO-induced injury size (% infarct volume) evaluated at 24 h post-dMCAO, was somewhat, but not significantly, smaller in PEMF-treated animals (15.8 %) as compared to controls (16.7 %) (MRI images on Figs. 2 and 3 and graph on Fig. 2). At 7 days, the infarct in PEMF animals was 14.9 vs 18.2 % in controls. In addition, at 7 days post-dMCAO, a significant edema was still present in control animals, while it was almost gone in PEMF-treated mice (Figs. 2 and 3). At 14 days, % infarct sizes in PEMF and control groups were 14.1 and 16.9 %, respectively. These differences were significant at 21 days, when the relative infarct volume (relative to volume of the intact hemisphere) in PEMF-treated animals was 11.65 %, which was 23.6 % smaller than the relative infarct volume (15.25 %) in control animals (Fig. 2, graph). Note visible differences in the extent of brain tissue damage between the two treatment groups at this time point (MRI images on Figs. 2 and 3; for better visualization, remaining normal brain tissue in the ipsilateral hemisphere is outlined with red dotted line).

Histological Evaluation of Infarct Size In order to verify our MRI results, following completion of the *in vivo* imaging at 21 days after dMCAO, the animals were subjected to heart perfusion, and the brains were

processed for tissue cryosectioning. Figure 4 demonstrates the representative histological images of thionine-stained serial coronal brain sections from the control and PEMF-treated animals. At 21 days, tissue loss and the lesioned hemisphere shrinkage were visibly greater in controls (remaining normal brain tissue is outlined with red dotted lines). The calculations revealed that the relative infarction volume in the ipsilateral hemisphere (expressed as a percentage of the volume of the control hemisphere) was 17.4 % in control animals and 10 % in PEMF-treated animals. These results are in agreement with our *in vivo* MRI measurements at 21 days (15.25 and 11.65 %, respectively). The minor differences between the *in vivo* MRI and histological measurements are associated with significant deformation of the brain tissue following fixation, freezing, and slicing procedures.

Effect of PEMF on Cytokine Expression Profile Following Cortical Ischemia

Since PEMF treatment reportedly has an anti-inflammatory action [15], we hypothesized that decreased infarct size could be attributed to reduction of postischemic inflammation. In this study, we focused mainly on the inflammation process during the post-acute phase of stroke. Dynamic changes in

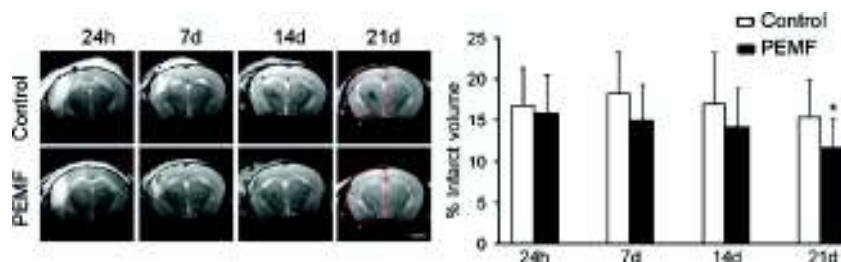
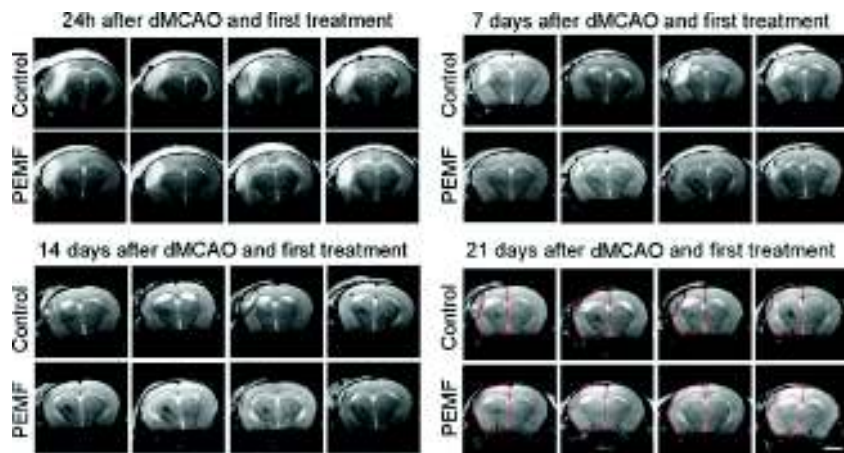


Fig. 2 PEMF treatment significantly reduces the infarct size at 21 days following dMCAO. T2-weighted MRI-based measurements of the infarct volume were done at 2, 14, and 21 days post-dMCAO. The brain damage progressed from vasogenic edema at 24 h post-dMCAO to tissue resorption at 21 days. *Bar*, 2 mm. The volumes of normal gray matter in the lesioned and nonlesioned control hemispheres were calculated, and the infarction volume was expressed as a percentage of the volume of the

gray matter in the control hemisphere. At 21 days after dMCAO, the necrotic tissue disappears due to tissue resorption. Assessment of the remaining normal brain tissue (outlined by red dotted lines) is especially helpful at this time point. % Infarct sizes in control (*white bars*) and PEMF-treated (*black bars*) were plotted on the graph ($N=12$ per group, Standard Deviation, $*p<0.05$, student's *t* test)

Fig. 3 Representative MRI images acquired from different PEMF-treated and four different control animals, demonstrate progression of the brain damage from 24 h to 7, 14, and 21 days after dMCAO. Note visible differences in infarct sizes between control and PEMF-treated animals. In the micrographs representing MRI measurements at 21 days after stroke, the remaining normal brain tissue in the lesioned hemispheres is outlined by red dotted line. Bar, 2 mm



cytokine profiles after stroke happen very rapidly: based on the literature reports, pro-inflammatory cytokine expression increases within several minutes (during an acute phase of stroke), peaks at 3–4 days, and remains elevated within 7 days [5]. Therefore, in order to detect any meaningful differences in cytokine expressions during the subacute phase, we had chosen two different time points of 4 days (initial regeneration period) and 7 days (progressive regeneration period) after stroke. In addition, we wanted the PEMF treatment to last for the same time period of 4 days, in both cases. To achieve this, two different treatment/assessment time points were used in these studies: (1) when PEMF treatment was initiated immediately (within 30–45 min) after dMCAO, and cytokine/chemokine expression was evaluated at 4 days after dMCAO; and (2) when PEMF treatment was initiated at 3 days after dMCAO, and cytokine/chemokine expression was evaluated at 7 days after dMCAO. The levels of pro- and anti-inflammatory factors were assessed in the dMCAO-damaged hemispheres, using specialized cytokines/chemokines PCR profiler array (Qiagen). This specialized array focused on the panel of pro-inflammatory molecules, includes common chemokines, cytokines as well as growth factors and

hormones with cytokine-like properties. Results obtained with the PCR array provide valuable information on the inflammation process in the injured brain tissue.

PEMF Treatment Was Initiated at 30–45 min After dMCAO, and Cytokine/Chemokine Expression Was Evaluated at 4 Days After dMCAO

Figure 5 and Table 1 demonstrate that at 4 days after dMCAO and PEMF treatment, there was a significant (≥ 1.5) upregulation of eight and downregulation of four cytokine genes. The fold changes of the upregulated (orange) and downregulated (violet) genes in PEMF-treated animals, as compared with controls, are plotted on the graph. Among the upregulated cytokines, six are known to have a dual (both pro- and anti-inflammatory, green star) effect, and two are pro-inflammatory (blue stars). Most of the downregulated cytokines have pro-inflammatory action; more importantly, gene encoding IL-1 α , the cytokine known to have a detrimental effect on poststroke outcome, was significantly reduced. We can conclude that PEMF treatment results in downregulation of pro-inflammatory cytokines, but it does not upregulate

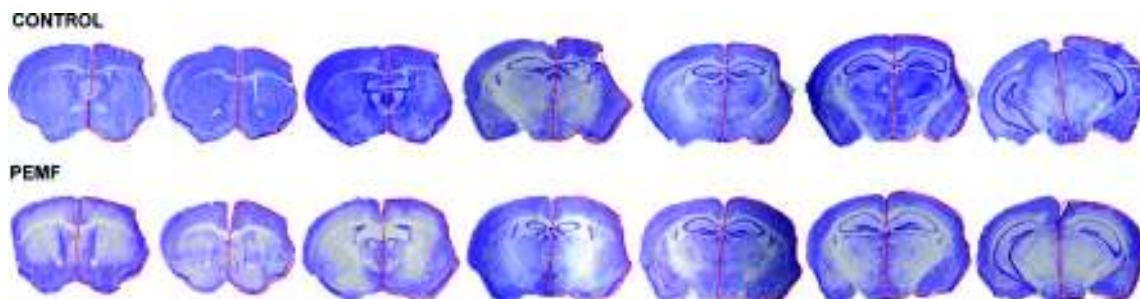


Fig. 4 Representative histological images of thionine-stained serial coronal brain sections. At 21 days after dMCAO, PEMF-treated and control animals were subjected to heart perfusion, and the brains were processed for tissue cryosectioning. Serial coronal sections were stained with thionine and imaged using Zeiss stereomicroscope and AxioVision software. Since at this time point following dMCAO there is a significant resorption

(loss) of the necrotic tissue, the lesion volume was measured according to the indirect method by assessing the size differences between the remaining ipsilateral (outlined by red dotted line) and unlesioned contralateral hemispheres. At 21 days, tissue loss and the lesioned hemisphere shrinkage were visibly greater in controls, as compared with PEMF-treated animals. Bar, 2 mm

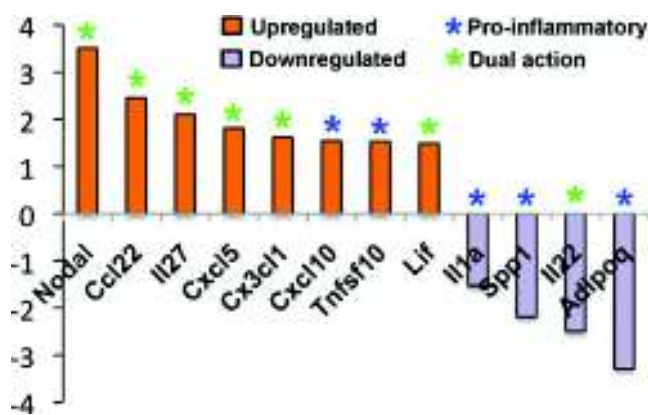


Fig. 5 Cytokine/chemokine gene expression in PEMF-treated mouse brains at 4 days after dMCAO. RNAs from PEMF-treated and control brains (cortices from the hemisphere ipsilateral to the lesion) were subjected to mouse cytokines/chemokines PCR profiler array (Qiagen). PEMF treatment resulted in a significant (ranging between 1.5- and 3.5-fold) increase (orange bars) or decrease (violet bars) in the expression levels of genes encoding cytokines and chemokines of pro-inflammatory (blue stars) or dual (both pro- and anti-inflammatory, green stars) action

clearly anti-inflammatory cytokines at the early stage of the poststroke recovery.

PEMF Treatment Was Initiated at 3 Days After dMCAO, and Cytokine/Chemokine Expression Was Evaluated at 7 Days After dMCAO

Figure 6 and Table 2 show that PEMF treatment resulted in a significant upregulation of 11 and downregulation of 19 genes. Among the downregulated genes, most of them encode

pro-inflammatory factors. It is important that similar to 4-day time period, we detected significant reduction of pro-inflammatory factors IL-1 α , adiponectin, and osteopontin at 7 days after stroke. It is very important to note that among the downregulated factors are three members of the major apoptosis-inducing tumor necrosis factor (TNF) superfamily, including FasL, Tnf, and Tnfsf13 β . Among the upregulated genes, 5 encode anti-inflammatory factors (red stars), including a major inflammation suppressor IL-10; three of the genes with increased expression have dual (green stars), and three pro-inflammatory (blue stars) effect. Interestingly, in PEMF-treated animals, pro-inflammatory chemokine Cxcl10 was upregulated at 4 days but downregulated at 7 days after stroke. A complete list of the affected genes, their fold changes and attributed functions are shown on Fig. 6 and Table 2. PCR array analysis results indicate that PEMF treatment leads to a stronger suppression of inflammation and apoptosis at later stages of poststroke recovery, as compared to early time point. Overall, we can conclude that PEMF significantly affects poststroke inflammation by suppressing major pro-inflammatory and overexpressing major pro-inflammatory factors.

Discussion

Our study demonstrates that PEMF treatment results in significantly decreased infarct size at 21 days following dMCAO-induced cortical ischemia, indicating possible long-term improvement of poststroke regeneration process. Our

Table 1 Effect of PEMF on cytokine/chemokine gene profile analyzed at 4 days after dMCAO

Gene	Fold change (PEMF vs control)	Description
Nodal	3.5129	Nodal (functions to control the survival, growth, differentiation and effector function of tissues and cells) [23]
Ccl22	2.4555	C-C motif chemokine 22 (displays chemotactic activity for monocytes, dendritic cells, natural killer cells and activated T lymphocytes)
Il27	2.1033	Interleukin 27 (new findings indicating anti-inflammatory action of IL27) [24, 25]
Cxcl5	1.8142	Chemokine ligand 5 (implicated in connective tissue remodeling)
Cx3cl1	1.62	Chemokine (C-X3-C motif) ligand 1 (promotes neuronal survival and inhibits microglial apoptosis) [26]
Cxcl10	1.5469	Chemokine ligand 10 (pro-inflammatory cytokine) [27]
Tnfsf10	1.5326	Tumor necrosis factor (ligand) superfamily, member 10 (preferentially induces apoptosis in transformed and tumor cells, but does not kill normal cells) [28]
Lif	1.4873	Leukemia inhibitory factor (promotes neuronal survival and differentiation) [29]
Il1a	-1.527	Interleukin 1 α (major pro-inflammatory protein) [30]
Spp1	-2.1845	Osteopontin (facilitates phagocytosis of neuronal debris by macrophages in the ischemic brain) [31, 32]
Il22	-2.4921	Interleukin 22, dual (both pro- and anti-inflammatory action) [33]
Adipoq	-3.2883	Adiponectin (associated with high mortality after stroke in human but was found to be neuroprotective after ischemia) [34]

Table shows the list of genes significantly (≥ 1.5 -fold) affected (increased or decreased expression) by PEMF treatment (also shown on Fig. 5). The table contains gene names (left row), their fold change (PEMF vs control, middle row), and respective encoded cytokines/chemokines and their functions (right row). Upregulated genes are shown in red, and downregulated genes are shown in blue

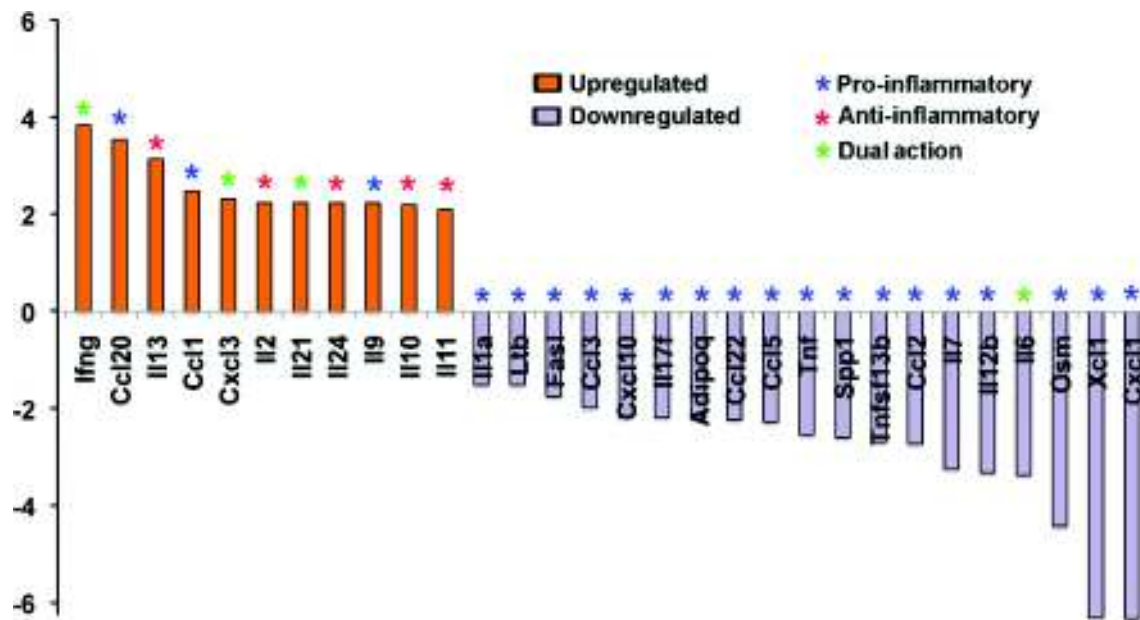


Fig. 6 Cytokine/chemokine gene expression in PEMF-treated mouse brains at 7 days after dMCAO. RNAs from PEMF-treated and control brains were subjected to mouse cytokines/chemokines PCR profiler array (Qiagen). PEMF treatment resulted in a significant (ranging between 1.5-

and 6-fold) increase (orange bars) or decrease (violet bars) in the expression of genes encoding cytokines and chemokines of pro-inflammatory (blue stars), dual (both pro- and anti-inflammatory, green stars) and anti-inflammatory (red stars) action

MRI data were in good agreement with histological measurements, which confirms the validity of our quantification approach. Reduction of the infarct size indicates that a larger volume of the brain tissue in the peri-infarct area of stroke (penumbra region) was rescued and prevented from necrosis and resorption. Decreased necrosis and thus, reduced neural cell death, could be attributed to the detected reduction in expression of genes encoding major pro-apoptotic members of the TNF superfamily (including Fas ligand, TNF, and TNFsf 13b). Significant (ranging from 1.7- to 2.7-fold) reduction of these factors at 7 days after stroke could considerably contribute to prevention of the brain tissue necrosis. At 21 days after dMCAO, PEMF-treated animals exhibited dramatic (4.4-fold) downregulation of *Osm* gene, encoding cytokine oncostatin, recently implicated as an inhibitor of adult neural stem cell proliferation [44]. Since proliferation of endogenous neural stem cells is critical in neurorestorative processes, downregulation of their inhibitor could have a very positive effect on neuroregeneration after stroke. PEMF signals are also implicated in modulation of calmodulin (CaM)-dependent nitric oxide (NO) signaling in many biological systems [45]. The role of NO in postischemic recovery is widely debated, and analysis of PEMF-induced NO modulation in our experimental model will be the subject of our future investigations. It was also demonstrated that preexposure with PEMF prior to ischemia and reperfusion results in the upregulation of protective stress protein *hsp70* gene and improvement of myocardial function [46]. We propose that in addition to these reported protective mechanisms, reduction in

infarct size detected in our study could be directly attributed to anti-inflammatory effect of PEMF.

Discussion on detrimental versus beneficial influence of inflammatory response on brain function remains unresolved. Many studies have reported beneficial effects of immunosuppressive manipulations on the stroke outcome. However, there is also evidence that the effect of particular components of the inflammatory cascade can be beneficial depending on the stage of tissue injury. Moreover, some pro-inflammatory cytokines and chemokines activate neuroprotective pathways as well as initiate neural stem cell migration and activation/differentiation [6, 8]. In our study, we focused on post-acute phase of cerebral ischemia and analyzed the effect of PEMF treatment at two different stages of poststroke recovery. At 4 days after dMCAO, the inflammation process was not significantly suppressed, but, rather, gently regulated. This might be beneficial because total suppression of inflammation would block the “positive” effect of the early inflammatory response such as initial activation of microglia, astrocytes, endogenous stem cells and immune cells, which contribute to brain tissue repair. The upregulation of cytokines with “dual” action demonstrates more fine-tuning, rather than aggressive action of the treatment. PCR array analysis results indicate that PEMF treatment leads to a stronger suppression of inflammation and apoptosis at later stages of poststroke recovery. This must be useful for the elimination of prolonged chronic inflammation, which would complicate the poststroke recovery process. Surprisingly, at 4 and 7 days post-dMCAO, PEMF had the opposite effect on the expression of *Cxcl10* gene: it was upregulated at 4 days, but downregulated at 7 days

Table 2 Effect of PEMF on cytokine/chemokine gene profile analyzed at 7 days after dMCAO

Gene	Fold change (PEMF vs control)	Description
Ifng	3.85	Interferon γ (dual role in inflammation) [35]
Ccl20	3.5504	Chemokine ligand 20 (pro-inflammatory, chemoattraction of immature dendritic cells T cells and B cells) [36]
Il13	3.15	Interleukin 13 (may have anti-inflammatory action) [37, 38]
Ccl1	2.4819	chemokine ligand 1 (pro-inflammatory chemokine)
Cxcl3	2.32	chemokine ligand 3 (possible dual role)
Il2	2.24	Interleukin 2 (anti-inflammatory action) [39]
Il21	2.24	Interleukin 21 (possible dual role)
Il24	2.24	Interleukin 24 (IL10 family of cytokines, may have anti-inflammatory action) [40]
Il9	2.24	Interleukin 9 (pro-inflammatory cytokine)
Il10	2.21	Interleukin 10 (anti-inflammatory cytokine) [38, 39]
Il11	2.11	Interleukin 11 (anti-inflammatory, may have therapeutic potential to prevent ischemic injury) [38, 40]
Il1a	-1.5	Interleukin 1 α (major pro-inflammatory cytokine implicated in pathogenesis of brain ischemia) [30]
Ltb	-1.5	Lymphotoxin β (pro-inflammatory action)
FasL	-1.74	Fas ligand (TNF superfamily, pro-apoptotic action) [41, 42]
Ccl3	-1.97	Chemokine ligand 3 (pro-inflammatory cytokine)
Cxcl10	-2.17	Chemokine ligand 10 (pro-inflammatory cytokine) [27]
Il17f	-2.17	Interleukin 17f (pro-inflammatory chemokine)
Adipoq	-2.19	Adiponectin (associated with high mortality after stroke but was found to be neuroprotective after ischemia) [34]
Ccl22	-2.22	Chemokine ligand 22 (pro-inflammatory chemokine)
Ccl5	-2.27	Chemokine ligand 5 (pro-inflammatory chemokine)
Tnf	-2.53	Tumor necrosis factor (TNF, pro-apoptotic action) [41, 42]
Spp1	-2.59	Osteopontin (facilitates phagocytosis of neuronal debris by macrophages in the ischemic brain) [31, 32]
Tnfsf13b	-2.68	Tumor necrosis factor superfamily 13 β (pro-apoptotic action) [41, 42]
Ccl2	-2.72	Chemokine ligand 2 (pro-inflammatory chemokine)
Il7	-3.24	Interleukin 7 (pro-inflammatory cytokine)
Il12b	-3.31	Interleukin 12 β (pro-inflammatory cytokine)
Il6	-3.36	Interleukin 6 (pro-inflammatory cytokine, may have dual action) [38, 43]
Osm	-4.41	Oncostatin (IL6 family cytokine, inhibits proliferation of adult neural stem cells) [44]
Xcl1	-6.30	Chemokine ligand 1 (pro-inflammatory chemokine)
Cxcl1	-6.33	Chemokine ligand 1 (pro-inflammatory chemokine)

Table shows the list of genes significantly (≥ 1.5 -fold) affected (decreased or increased expression) by PEMF treatment (also shown on Fig. 6). The table contains gene names (left row), their fold change (PEMF vs control, middle row), and respective encoded cytokines/chemokines and their functions (right row). Upregulated genes are shown in red, and downregulated genes are shown in blue

after stroke. This once more demonstrates complexity of the cytokine function, and their either “beneficial” or “harmful” role at different stages after injury. Our results are in agreement with the reported differential effect of magnetic fields on pro- and anti-inflammatory cytokine expression during initial and sustained inflammatory response, at different stages of wound healing [47]. We can conclude that PEMF provides a moderate reduction of inflammation on the early stages and a stronger suppression of the inflammation process at later stages of poststroke recovery. More importantly, PEMF treatment has a consistent suppressive effect on inflammation: it significantly reduces major pro-inflammatory IL-1 α gene expression, and at the same time, upregulates major pro-

inflammatory IL-10. The results obtained in this study confirm the anti-inflammatory action of PEMF reported in wide range of clinical studies [14–17].

In summary, based on the wide variety of literature it is evident that a growing number of patients have received clinical benefit from PEMF treatment, and new clinical indications of its beneficial effects are emerging. We propose that PEMF treatment may be potentially utilized as a noninvasive and long-lasting adjunctive treatment during recovery after stroke. We demonstrated that PEMF application has positive effects on neuroinflammation even if it is initiated as late as 3 days after stroke; this might be of special interest for clinicians since patients often receive medical treatment within

several hours to several days after the onset of stroke. Potential benefits of PEMF as adjunctive treatment may include preservation of cerebral tissue in the penumbral area, as well as regulation of inflammation and neurorestoration after the stroke-related brain injury.

Acknowledgments This work was supported in part by Ivivi Health Sciences, LLC. We would like to thank Dr. Arthur Pilla for his valuable input and assistance. Microscopy images were generated in the UNM Cancer Center Fluorescence Microscopy Facility supported as detailed on the webpage <http://hsc.unm.edu/crtc/microscopy/instru.html>. Gene and miRNA analysis was performed in the Keck-UNM Genomics Resource (KUGR) facility and in Qiagen Company.

Conflict of Interest Juan Carlos Pena-Philippides has no financial interest with the sponsor of the research. Yirong Yang has no financial interest with the sponsor of the research. Olga Bragina has no financial interest with the sponsor of the research. Sean Hagberg has financial interests with Ivivi Health Sciences. Edwin Nemoto has no financial interest with the sponsor of the research. Tamara Roitbak has no financial interest with the sponsor of the research.

References

- American Heart Association <http://www.americanheart.org/presenter.jhtml?identifier=4725>. 2010.
- Statistics NY-PD <http://nyp.org/health/disability-statistics.html>. 2010.
- Brouns R, De Deyn PP. The complexity of neurobiological processes in acute ischemic stroke. *Clin Neurol Neurosurg*. 2009;111(6):483–95. doi:10.1016/j.clineuro.2009.04.001.
- Lucas SM, Rothwell NJ, Gibson RM. The role of inflammation in CNS injury and disease. *Br J Pharmacol*. 2006;147 Suppl 1:S232–40. doi:10.1038/sj.bjp.0706400.
- Perera MN, Ma HK, Arakawa S, Howells DW, Markus R, Rowe CC, et al. Inflammation following stroke. *J Clin Neurosci*. 2006;13(1):1–8. doi:10.1016/J.Jocn.2005.07.005.
- Liguz-Leczna M, Kossut M. Influence of inflammation on poststroke plasticity. *Neural Plast*. 2013;2013:258582. doi:10.1155/2013/258582.
- Lakhan SE, Kirchgessner A, Hofer M. Inflammatory mechanisms in ischemic stroke: therapeutic approaches. *J Transl Med*. 2009;7:97. doi:10.1186/1479-5876-7-97.
- Russo I, Barlati S, Bosetti F. Effects of neuroinflammation on the regenerative capacity of brain stem cells. *J Neurochem*. 2011;116(6):947–56. doi:10.1111/j.1471-4159.2010.07168.x.
- Pilla AA. Nonthermal electromagnetic fields: from first messenger to therapeutic applications. *Electromagn Biol Med*. 2013;32(2):123–36. doi:10.3109/15368378.2013.776335.
- Grant G, Cadossi R, Steinberg G. Protection against focal cerebral ischemia following exposure to a pulsed electromagnetic field. *Bioelectromagnetics*. 1994;15(3):205–16.
- Sandyk R. Alzheimer's disease: improvement of visual memory and visuoconstructive performance by treatment with picotesla range magnetic fields. *Int J Neurosci*. 1994;76(3–4):185–225.
- Sandyk R. Brief communication: electromagnetic fields improve visuospatial performance and reverse agraphia in a Parkinsonian patient. *Int J Neurosci*. 1996;87(3–4):209–17.
- Mizushima Y, Akaoka I, Nishida Y. Effects of magnetic field on inflammation. *Experientia*. 1975;31(12):1411–2.
- Rasouli J, Lekhraj R, White NM, Flamm ES, Pilla AA, Strauch B, et al. Attenuation of interleukin-1beta by pulsed electromagnetic fields after traumatic brain injury. *Neurosci Lett*. 2012;519(1):4–8. doi:10.1016/j.neulet.2012.03.089.
- Rohde C, Chiang A, Adipoju O, Casper D, Pilla AA. Effects of pulsed electromagnetic fields on interleukin-1 beta and postoperative pain: a double-blind, placebo-controlled, pilot study in breast reduction patients. *Plast Reconstr Surg*. 2010;125(6):1620–9.
- Heden P, Pilla AA. Effects of pulsed electromagnetic fields on postoperative pain: a double-blind randomized pilot study in breast augmentation patients. *Aesthet Plast Surg*. 2008;32(4):660–6. doi:10.1007/s00266-008-9169-z.
- Nelson FR, Zvirbulis R, Pilla AA. Noninvasive electromagnetic field therapy produces rapid and substantial pain reduction in early knee osteoarthritis: a randomized double-blind pilot study. *Rheumatol Int*. 2013;33(8):2169–73. doi:10.1007/s00296-012-2366-8.
- Kuraoka M, Furuta T, Matsuwaki T, Omatsu T, Ishii Y, Kyuwa S, et al. Direct experimental occlusion of the distal middle cerebral artery induces high reproducibility of brain ischemia in mice. *Exp Anim*. 2009;58(1):19–29.
- Swanson RA, Morton MT, Tsao-Wu G, Savalos RA, Davidson C, Sharp FR. A semiautomated method for measuring brain infarct volume. *J Cereb Blood Flow Metab*. 1990;10(2):290–3. doi:10.1038/jcbfm.1990.47.
- Jones PB, Shin HK, Boas DA, Hyman BT, Moskowitz MA, Ayata C, et al. Simultaneous multispectral reflectance imaging and laser speckle flowmetry of cerebral blood flow and oxygen metabolism in focal cerebral ischemia. *J Biomed Opt*. 2008;13(4):044007. doi:10.1117/1.2950312.
- Carmichael ST. Rodent models of focal stroke: size, mechanism, and purpose. *NeuroRx*. 2005;2(3):396–409. doi:10.1602/neurorx.2.3.396.
- Wiessner C, Allegrini PR, Ekatodramis D, Jewell UR, Stallmach T, Gassmann M. Increased cerebral infarct volumes in polyglobulic mice overexpressing erythropoietin. *J Cereb Blood Flow Metab*. 2001;21(7):857–64. doi:10.1097/00004647-200107000-00011.
- Shen MM. Nodal signaling: developmental roles and regulation. *Development*. 2007;134(6):1023–34. doi:10.1242/dev.000166.
- Wojno ED, Hunter CA. New directions in the basic and translational biology of interleukin-27. *Trends Immunol*. 2012;33(2):91–7. doi:10.1016/j.it.2011.11.003.
- Hall AO, Silver JS, Hunter CA. The immunobiology of IL-27. *Adv Immunol*. 2012;115:1–44. doi:10.1016/B978-0-12-394299-9.00001-1.
- Cardona AE, Pioro EP, Sasse ME, Kostenko V, Cardona SM, Dijkstra IM, et al. Control of microglial neurotoxicity by the fractalkine receptor. *Nat Neurosci*. 2006;9(7):917–24. doi:10.1038/nn1715.
- Gotsch F, Romero R, Friel L, Kusanovic JP, Espinoza J, Erez O, et al. CXCL10/IP-10: a missing link between inflammation and anti-angiogenesis in preeclampsia? *J Matern-Fetal Neonatal Med*. 2007;20(11):777–92. doi:10.1080/14767050701483298.
- Pan W, Kastin AJ. Tumor necrosis factor and stroke: role of the blood-brain barrier. *Prog Neurobiol*. 2007;83(6):363–74. doi:10.1016/j.pneurobio.2007.07.008.
- Slevin M, Krupinski J, Mitsios N, Perikleous C, Cuadrado E, Montaner J, et al. Leukaemia inhibitory factor is over-expressed by ischaemic brain tissue concomitant with reduced plasma expression following acute stroke. *Eur J Neurol*. 2008;15(1):25–33. doi:10.1111/J.1468-1331.2007.01995.X.
- Boutin H, LeFeuvre RA, Horai R, Asano M, Iwakura Y, Rothwell NJ. Role of IL-1(alpha) and IL-1(beta) in ischemic brain damage (vol 21, pg 5528, 2001). *J Neurosci*. 2001;21(17):U11–U.
- Ellison JA, Velier JJ, Spera P, Jonak ZL, Wang XK, Barone FC, et al. Osteopontin and its integrin receptor alpha(V)beta(3) are upregulated

- during formation of the glial scar after focal stroke. *Stroke*. 1998;29(8):1698–706.
32. Wang X, Loudon C, Yue TL, Ellison JA, Barone FC, Solleveld HA, et al. Delayed expression of osteopontin after focal stroke in the rat. *J Neurosci*. 1998;18(6):2075–83.
 33. Rutz S, Eidenschenk C, Ouyang WJ. IL-22, not simply a Th17 cytokine. *Immunol Rev*. 2013;252:116–32. doi:10.1111/Imr.12027.
 34. Song W, Huo T, Guo F, Wang H, Wei H, Yang Q, et al. Globular adiponectin elicits neuroprotection by inhibiting NADPH oxidase-mediated oxidative damage in ischemic stroke. *Neuroscience*. 2013;248C:136–44. doi:10.1016/j.neuroscience.2013.05.063.
 35. Muhl H, Pfeilschifter J. Anti-inflammatory properties of pro-inflammatory interferon-gamma. *Int Immunopharmacol*. 2003;3(9):1247–55. doi:10.1016/S1567-5769(03)00131-0.
 36. Schutyser E, Struyf S, Van Damme J. The CC chemokine CCL20 and its receptor CCR6. *Cytokine Growth Factor Rev*. 2003;14(5):409–26.
 37. Watson ML, White AM, Campbell EM, Smith AW, Uddin J, Yoshimura T, et al. Anti-inflammatory actions of interleukin-13: suppression of tumor necrosis factor-alpha and antigen-induced leukocyte accumulation in the guinea pig lung. *Am J Respir Cell Mol Biol*. 1999;20(5):1007–12. doi:10.1165/ajrcmb.20.5.3540.
 38. Opal SM, DePalo VA. Anti-inflammatory cytokines. *Chest*. 2000;117(4):1162–72.
 39. Banachereau J, Pascual V, O'Garra A. From IL-2 to IL-37: the expanding spectrum of anti-inflammatory cytokines. *Nat Immunol*. 2012;13(10):925–31. doi:10.1038/ni.2406.
 40. Cuneo AA, Autieri MV. Expression and function of anti-inflammatory interleukins: the other side of the vascular response to injury. *Curr Vasc Pharmacol*. 2009;7(3):267–76.
 41. Vassalli P. The pathophysiology of tumor necrosis factors. *Annu Rev Immunol*. 1992;10:411–52. doi:10.1146/annurev.iy.10.040192.002211.
 42. Bodmer JL, Schneider P, Tschopp J. The molecular architecture of the TNF superfamily. *Trends Biochem Sci*. 2002;27(1):19–26.
 43. Gabay C. Interleukin-6 and chronic inflammation. *Arthritis Res Ther*. 2006;8. doi:10.1186/Ar1917.
 44. Beatus P, Jhaveri DJ, Walker TL, Lucas PG, Rietze RL, Cooper HM, et al. Oncostatin M regulates neural precursor activity in the adult brain. *Dev Neurobiol*. 2011;71(7):619–33. doi:10.1002/Dneu.20871.
 45. Pilla AA. Electromagnetic fields instantaneously modulate nitric oxide signaling in challenged biological systems. *Biochem Biophys Res Commun*. 2012;426(3):330–3. doi:10.1016/j.bbrc.2012.08.078.
 46. George I, Geddis MS, Lill Z, Lin H, Gomez T, Blank M, et al. Myocardial function improved by electromagnetic field induction of stress protein hsp70. *J Cell Physiol*. 2008;216(3):816–23. doi:10.1002/jcp.21461.
 47. Pesce M, Patrino A, Speranza L, Reale M. Extremely low frequency electromagnetic field and wound healing: implication of cytokines as biological mediators. *Eur Cytokine Netw*. 2013;24(1):1–10. doi:10.1684/ecn.2013.0332.